Macromolecular Research

Article

DOI 10.1007/s13233-019-7013-8

www.springer.com/13233 pISSN 1598-5032 eISSN 2092-7673

Interfacial Compression-Dependent Merging of Two Miscible Microdroplets in an Asymmetric Cross-Junction for *In Situ* Microgel Formation

Yeongseok Jang[†,1]
Chaenyung Cha[†,2]
Jinmu Jung[*,3]
Jonghyun Oh[*,3]

[1] Department of Mechanical Design Engineering, College of Engineering, Chonbuk National University, Jeonju, Jeonbuk 54896, Korea
[2] School of Materials Science and Engineering, Ulsan National Institute of Science and Technology (UNIST), Ulsan 44919, Korea
[3] Department of Nano-bio Mechanical System Engineering, College of Engineering, Chonbuk National University, Jeonju, Jeonbuk 54896, Korea

Received May 1, 2018 / Revised June 25, 2018 / Accepted June 26, 2018

Abstract: Controlling the merging of different microdroplets in a microfluidics system could generate a multitude of complex droplets because of their inherent surface tension, but poses a significant challenge because of their high surface tension. Here, a novel microfluidic merging technique is introduced using an asymmetric cross-junction geometry which increases the interfacial compression between two microdroplets. Microdroplets of two viscous polymer solutions, oxidized dextran (ODX) and *N*-carboxyethyl chitosan (N-CEC), which can undergo a crosslinking reaction *via* Schiff base formation, are allowed to merge at the asymmetric cross-junction without the assistance of additional merging schemes. The N-CEC and ODX microdroplets being formed at their orifices contact at a more favorable position to overcome their interfacial tension through this asymmetric geometry, until the interfacial layer breaks and pushes the former (with higher viscosity) into the latter. On the other hand, a typical symmetric cross-junction geometry cannot induce merging, because of insufficient interfacial compression generated by direct collision between two droplets. The merged N-CEC and ODX droplets soon become completely homogeneous *via* diffusion, ultimately leading to *in situ* microgel formation. Changing the concentration of ODX further controls the crosslinking density of the microgels. In addition, the viability of cells encapsulated within the microgels is well maintained, demonstrating the biocompatibility of the entire process. Taken together, the microfluidic merging technique introduced here could be broadly applicable for engineering cell-encapsulated microgels for biomedical applications.

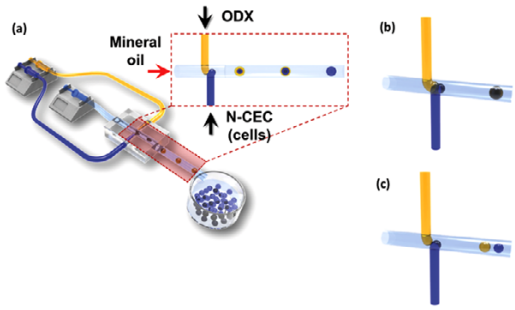

Keywords: *N*-carboxyethyl chitosan, oxidized dextran, microgel, droplet merging, asymmetric cross-junction.

1. Introduction

Rapid development in microfluidics in recent years has provided a valuable platform for engineering complex and microscale materials. In particular, droplet-based microfluidic techniques, such as single droplet formation,[1-3] double emulsion or high-order emulsions formation,[4-6] Janus droplet generation,[7,8] droplet manipulation,[9-12] droplet merging,[13-16] and droplet separation,[17,18] are now widely used to generate a variety of spherical particles with controllable dimensions for industrial applications as well as scientific investigation of fluid mechanics. In addition, its integration with biomedical (or biological) microelectromechanical systems ('Bio-MEMS') technology has expanded the role of microfluidics to the field of biomedical engineering, including drug delivery, tissue engineering and diagnostics.[19] For example, spherical microgels fabricated by crosslinking the gel-precursor droplets, generated by a flow-focusing microfluidic device, have been used as cell-culture platform and drug delivery systems.[20] More recently, droplet-based microfluidics has been applied in synthetic biology to reduce the dependence on expensive and labor-intensive liquid-handling robotics, leading to a better access for synthetic biologists to techniques that could provide improved reproducibility to engineer biological systems.[21]

An emerging technique in droplet-based microfluidics is the passive microdroplet merging, in which two microdroplets with different physical properties (*e.g.* viscosity, surface tension) are allowed to merge into a single droplet by controlling various microfluidic parameters, such as channel geometry, flow rate, droplet size, relative fluid viscosity, interfacial compression, and decompression. For example, the abacus-groove structure has been used for droplet-based addition and flow rate control without the use of surfactants.[22] Two droplets coming from opposing channels being merged and forced into another channel at the T-junction was able to induce the coalescence of confined droplets without surfactants.[23] In double emulsion, a widening channel followed by a narrower channel can decrease droplet velocity to realize droplet merging.[24-26] Alternatively in other

Acknowledgment: This work was supported by National Research Foundation of Korea (NRF) funded by the Ministry of Science and ICT (2016R1C1B2014747, 2017R1A4A1015681, and 2017M3A9C6033875).

***Corresponding Authors:** Jinmu Jung (jmjung@jbnu.ac.kr), Jonghyun Oh (jonghyuno@jbnu.ac.kr)
[†]These authors equally contributed to this work.

channels, a geometrical constriction has been applied to merge droplets with downstream merging of two droplets.[27,28]

A straight channel can be used to merge droplets by size or viscosity difference without surfactants.[29,30] Geometrical constriction and size differences for merging surfactant-covered droplets have been used in a co-flow channel system.[9,13,31] Also, a Y-shaped merging chamber was suggested for facilitating a two-step competition between hydrodynamic forces and surface tension in the absence of a surfactant.[32] This technique is deemed especially useful for the fabrication of *in situ* forming microgels for biomedical applications, by simply merging two polymer droplets that can undergo crosslinking reaction. Without the need for additional crosslinking procedure or toxic initiators further ensures the biocompatible encapsulation of biological species. However, for fluids with high viscosity, it is generally not possible to form droplets without the significant amount of surfactants. Therefore, these passive approaches are not enough to induce merging, and more active merging techniques are utilized.[33] For example, hydrostatic pressure along with synchronization reinjection is utilized to induce droplet merging.[34] Electric field has been employed to cause instantaneous instability of droplets to induce merging ('electrocoalescence').[35,36] Similarly, magnetic field also has been used to induce merging of droplets having ferroelectric properties.[37]

In this study, we suggest a new method for fabrication of *in situ* crosslinkable microdroplets by inducing the merging of two droplets with high and differing viscosities using an asymmetric cross-junction (Figure 1). For two microdroplets with high viscosities requiring a significant concentration of surfactant and with contrasting viscosities, it is difficult to merge the microdroplets by directly pushing against each other due to high surface tension. By intentionally adjusting the relative position of the two merging channels in the cross-junction ("asymmetric" position), one microdroplet with higher viscosity was allowed to contact the other microdroplet at a much reduced contact angle (*i.e.* reduced interfacial tension), facilitating the merging process by interfacial compression without the need for additional merging schemes. This merging method also has the advantage of not requiring the stoppage of the flow or droplets nor inclusion of droplets squeezing through additional narrow channels for compression and decompression. Immediately after the merging, the more viscous microdroplet was pushed into the center of the merged droplet, whereas the less viscous component acted as a cross-linker and surrounded the former. However, the merged droplets eventually became homogeneous *via* diffusion, with the subsequent *in situ* crosslinking reaction leading to microgel formation. The viability of the cells encapsulated in the microgels was further characterized to evaluate the biocompatibility of the material and the microfluidic merging process.

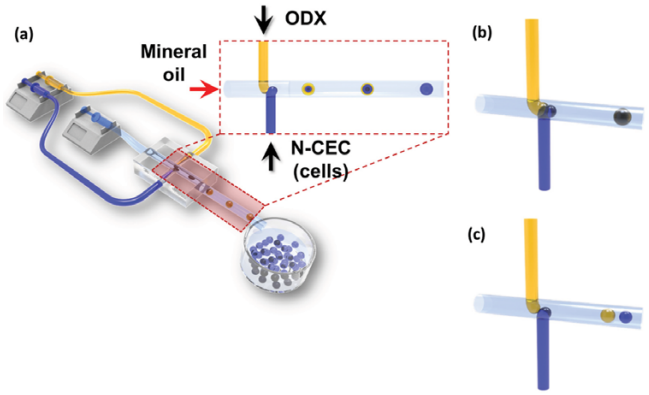

Figure 1. (a) Schematic diagram of the asymmetric junction used to generate the interfacial compression-dependent merging of the two miscible, surfactant-coated microdroplets; (b) the merging of the two miscible microdroplets by interfacial compression at reduced contact angles; and (c) separation of the two miscible microdroplets by contact mismatch.

2. Experimental

2.1. Materials

Water soluble *N*-carboxyethyl chitosan (N-CEC) was synthesized based on a modified protocol from a previously described method.[38,39] First, chitosan (Sigma Aldrich, MO, USA) was dispersed in 400 mL deionized water (DW) *via* stirring at 400 rpm. 5.6 mL of acrylic acid was then slowly added to the mixture, and continuously stirred for 48 h at 50 °C. After the reaction, the pH of the mixed solution was adjusted to 10-12 by the dropwise addition of a 0.1 M aqueous NaOH solution, converting the N-CEC into its sodium salt. To prepare the oxidized dextran (ODX), which contains multiple aldehyde groups capable of reacting with amine groups of N-CEC, 1.1 g of $NaIO_4$ was added to a 320 mL solution of 1.25% (w/v) dextran (Sigma-Aldrich, MO, USA) and stirred using a magnetic stirrer at a speed of 400 rpm for 48 h at room temperature under dark. Finally, by adding 2.5 g of ethylene glycol (Sigma-Aldrich, MO, USA) to the mixture, the unreacted $NaIO_4$ was quenched. Both the N-CEC and ODX solutions were extensively dialyzed using a dialysis membrane (MWCO 12000) in DW for 3 days, and lyophilized to obtain the final products.

2.2. Cell culture

NIH-3T3 fibroblasts (mouse embryonic fibroblast cell line) were cultured in Dulbecco's modified Eagle's medium (DMEM, high glucose, Invitrogen, NY, USA). The DMEM contained 1% penicillin-streptomycin (Invitrogen, NY, USA) and 10% fetal bovine serum (FBS, Invitrogen, NY, USA). The cells were incubated in a humidified atmosphere with 5% CO_2 at 37 °C. The media was changed every 2 days and the cells were passaged every 3 days. The NIH-3T3 cells were prepared at a concentration of 10^7 cells per mL. Then, they were gently dispersed in 3% (w/v) N-CEC solution, which would be later infused into an asymmetric inlet of the microfluidic device.

2.3. Fabrication of a microfluidic device with asymmetric cross-junction

Figure 1 shows the schematic illustration of the asymmetric microfluidic channels used to generate the two miscible microdroplets. The microfluidic device consisted of three inlets and one outlet. One horizontal inlet was used to introduce mineral

oil (M5904; Sigma Aldrich, St. Louis, MO, USA). The other two inlets located perpendicular to each other were used to infuse the N-CEC and ODX solutions. The inlets were fabricated using glass capillaries (World Precision Instruments, Inc. FL, USA) with a 580 μm inner diameter (ID). The outlet for the generated microdroplets was also composed of a glass capillary (580 μm ID). The use of glass capillaries in microfluidic channels is beneficial because of the high chemical resistance and controllable surface wettability of the glass material. To seal the glass capillary-based inlets and outlet, a polydimethylsiloxane (PDMS) block was prepared by mixing a silicone elastomer base with its curing agent (Sylgard184 silicone elastomer kit; Dow Corning, Midland, MI, USA) at a ratio of 10 to 1. The mixture was cured at 80 °C for 2 h. Grooves to embed the glass capillaries were carved on the PDMS block. All capillaries were placed on a glass slide (25×75 mm) and fixed using an epoxy resin. The PDMS block was treated with plasma discharge (Harrick Plasma, Ithaca, NY, USA), and permanently bonded to the glass capillaries with a slide glass. The three inlets were connected with two syringe pumps (Harvard Apparatus, MA, USA) *via* Tygon tubes. The N-CECS and ODX solutions, and mineral oil were loaded with three separate 5 mL syringes.

2.4. Generation of *in situ* forming microgels

The microfluidic device with an asymmetric cross-junction shown in Figure 1 was used to generate *in situ* forming microgels by merging ODX and N-CEC microdroplets. Through the two asymmetric inlets, 3% (w/v) N-CEC and 2% or 4% (w/v) ODX solutions were introduced at a constant flow rate of 30 μL/h. Mineral oil, supplemented with 20 wt% emulsifier (Span 80, Sigma Aldrich, MO, USA) was infused through the other horizontal inlet at a constant flow rate of 50 μL/h. The high concentration of Span 80 at 20% (w/v) was necessary for stable droplet generation due to the high viscosities of the two solutions.[20,40,41] In the prepared microfluidic system, mineral oil was used as the continuous phase, while the N-CEC and ODX solutions acted as the dispersed solutions. Initially, as the ODX solution was perfused through the front asymmetric inlet, it came into contact with the mineral oil. As a result, the ODX solution was compressed by the induced shearing force, and monodispersed microdroplets began to form. Before the ODX microdroplet was fully formed and detached from the inlet, N-CEC microdroplet was generated in the opposite rear asymmetric inlet. As the size of two N-CEC and ODX microdroplets gradually grew, the two miscible microdroplets contacted each other with an initial contact angle. The initial contact angle between the two miscible microdroplets changed as the size of the two microdroplets increased. Then, the two miscible microdroplets merged due to the interfacial compression overcoming their surface tension. With the merged microdroplets becoming homogeneous with diffusion, the *in situ* gelation occurred without additional crosslinking efforts. To fabricate the cell-encapsulated microgels, NIH-3T3 fibroblasts were dispersed in the N-CEC and ODX solutions prior to the microfluidic processing. The entire procedure was monitored and recorded using an inverted optical microscope (Olympus, Tokyo, Japan).

2.5. Rheological measurement

The N-CEC and ODX solutions in phosphate-buffered saline (PBS, pH 7.4) were prepared. The concentration of N-CEC was kept at 3% (w/v), while the concentration of ODX was controlled at either 2 or 4% (w/v). To characterize the rheological behavior of the two solutions, their viscosities were measured using a rotating viscometer (AR-G2, TA Instruments Ltd, Crawley, UK). The lower plate was fixed, and the upper plate was rotated at a specific strain under the stress-controlled mode. All measurements were performed at 25±0.1 °C. The non-Newtonian behavior of the two solutions was characterized by measuring their viscosities over a shear rate ranging from 1 to 100 s^{-1}. It should be noted that a non-Newtonian fluid is defined as a fluid which shows different viscosities as the shear rate changes. The obtained viscosity results were represented in a log scale on the x-axis (shear rate) and a decimal scale on the y-axis (viscosity) and were performed in triplicate.

The capillary numbers (Ca) and Reynolds numbers (Re) of N-CEC and ODX were calculated using the following equations,

$$\mathrm{Ca} = \frac{\mu \upsilon}{\sigma} \tag{1}$$

$$\mathrm{Re} = \frac{\rho \upsilon L}{\mu} \tag{2}$$

where μ was the dynamic viscosity (0.02 Pa·s for ODX, 0.12 Pa·s for N-CEC), υ was the velocity (1.1565×10^{-4} m·s^{-1}), ρ was the density (1,010 kg·m^{-3} for ODX, 992 kg·m^{-3} for N-CEC), and σ was the surface tension (0.07 N·m^{-1} for ODX, 0.043 N·m^{-1} for N-CEC). L was the characteristic length (5.8×10^{-4} m).[42] Ca values for ODX and N-CEC were 3.3×10^{-5} and 3.23×10^{-4}, respectively, while Re values for ODX and N-CEC were 1.3×10^{-3} and 2.1×10^{-3}, respectively.

2.6. Contact angle measurement

As the N-CEC and ODX solutions were introduced through the asymmetric inlets, the generation of two monodispersed microdroplets was recorded using a real-time microscopic camera. The snapshot images at different time points were taken from a video and the contact angles were measured using the obtained images. When the two miscible monodispersed microdroplets first contacted each other, an initial contact angle between the two microdroplets was determined. The change in contact angle between the two microdroplets was subsequently analyzed until they merged into a single microdroplet.

Surface tension (σ) of the microdroplets during the merging process was calculated using the curvature parameters (d_s and d_e) of a droplet,

$$\sigma = \frac{\Delta \rho g d_e^2}{H} \tag{3}$$

where ρ is the density difference of the droplet from the surrounding, g is the gravitational acceleration (9.8 m s^{-2}), d_e is the width of the droplet, and H is a dimensionless parameter related to the shape-dependent variable $S=d_s/d_e$.[43,44]

2.7. Cell viability test

The viability of the NIH-3T3 cells encapsulated in the microgels was investigated using a LIVE/DEAD® Viability Cytotoxicity Kit (Invitrogen, NY, USA). Briefly, cell-encapsulated microgels, incubated in the cell culture medium at 37 °C, were collected and stained with calcein-AM (0.5 μL/mL; green fluorescence) and the ethidium homodimer-1 (2 μL/mL; red fluorescence) to allow fluorescent visualization of live and dead cells, respectively. The images of fluorescently-labeled cells were observed and taken using a fluorescence microscope equipped with a CCD camera. The number of live and dead cells were counted in ten different spherical microgels, and the mean and standard deviation values were reported.

3. Results and discussion

3.1. Rheological properties of ODX and N-CEC solutions

The viscosities of the ODX and N-CEC solutions were first measured to assess their fluid behavior under varying shear stress (Figure 2). The shear rate was controlled from 1 to 100 s^{-1}. The viscosities of the 3% (w/v) N-CEC solution was observed to be 162.0, 117.2, and 104.5 cP at shear rates of 1, 10, and 100 s^{-1}, respectively, clearly demonstrating the non-Newtonian (shear-thinning) behavior. The 2% (w/v) ODX solution also showed decrease in viscosity with shear rate, although the values were generally much lower than the N-CEC solution (*e.g.* 49.2, 25.0, and 19.0 cP at the same shear rates). Increasing the concentration of ODX solution to 4% (w/v) did not result in a significant change in viscosity at the same range of shear rate. This shear-thinning behavior of both solutions suggested that the formation of microdroplets and the control of their morphology could be attained by the shear stress induced by the microfluidic flow. In addition, the N-CEC microdroplet having much higher viscosity could drive enough compression onto the less viscous ODX microdroplet for efficient merging process. The capillary numbers of N-CEC was an order of magnitude higher than that of ODX, which further illustrated the greater effect of high viscosity for N-CEC.

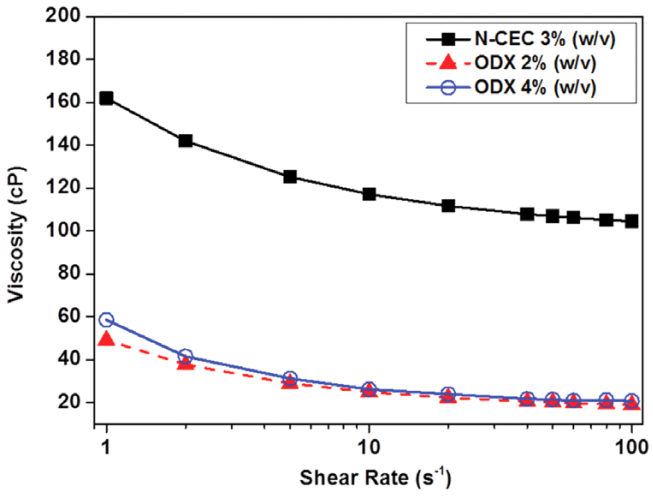

Figure 2. Viscosity profile of the 3% (w/v) N-CEC and 2% and 4% (w/v) ODX solutions at a shear rate ranging from 1 to 100 s^{-1}, showing clear non-Newtonian behavior.

It should be noted here that the concentration of N-CEC at 3% (w/v) was chosen so as to induce gelation with ODX below 5% (w/v); at lower concentrations of N-CEC, higher concentration of ODX was required to form microgels, which would significantly increase the viscosity of ODX and thus rendering it difficult to merge two microdroplets with higher viscosity. In addition, due to the extremely high viscosity of N-CEC above 3% (w/v), the concentration of N-CEC above 3% (w/v) was not further explored. The lower limit of ODX was chosen as 2% (w/v) below which the gelation did not occur.

3.2. Microdroplet merging by microfluidic device with asymmetric cross-junction

Figure 3 shows the optical microscopic images of the merging of the two microdroplets at the asymmetric cross-junction. In Figure 3(a), two miscible microdroplets made from the 3% (w/v) N-CEC and 2% (w/v) ODX solutions were introduced through the asymmetric inlets. It should be noted that the 2% (w/v) and 4% (w/v) ODX solutions showed no significant difference in generating the merged microdroplets, as indicated by the similar viscosity values in Figure 2. As the diameter of the two droplets increased, they started to contact each other, as can be seen in Figure 3(b). The initial contact angle between the 3% (w/v) N-CEC and 2% (w/v) ODX solutions was 173°. As the size of the two miscible microdroplets grew, the contact angle decreased from 173° to 158°, as shown in Figures 3(c)-(e), indicating the increased interfacial compression between the two microdroplets. The N-CEC microdroplets having higher viscosity became spherical more quickly and thus possessed greater surface tension, while the ODX microdroplet was more slowly being formed due to lower viscosity. This allowed the N-CEC microdroplet to push the ODX microdroplet at a much reduced interfacial tension. When the two microdroplets eventually reached the critical contact angle of 158°, they merged forming a larger microdroplet (Figure 3(f)). The decrease in contact angle at the interface as well as the change in curvature of the microdroplets indicates the decrease in surface tension.[43] The calculated surface tension values are shown in Figure 3(g). This phenomenon demonstrated that the sufficient amount of compression caused by the converging of the two fluids, as identified with the decreasing contact angle, was needed to break the interfacial tension between the two microdroplets.

It is critical to note that the merging of two microdroplets was only possible using the asymmetric cross-junction, and the merging did not occur when the symmetric cross-junction (*i.e.* two channels are aligned) was instead used (Figure 4). At the symmetric cross-junction, the two microdroplets being formed pushed each other head-on, so the area of contact is small and the duration of the contact was too short to apply enough compression for the microdroplets to merge, resulting in the microdroplets separately flowing past without merging (Figure 4(a)). This difficulty in merging is especially more inclined to occur for high viscosity fluids undergoing laminar flow, as identified by their low Reynolds numbers. At the asymmetric cross-junc-

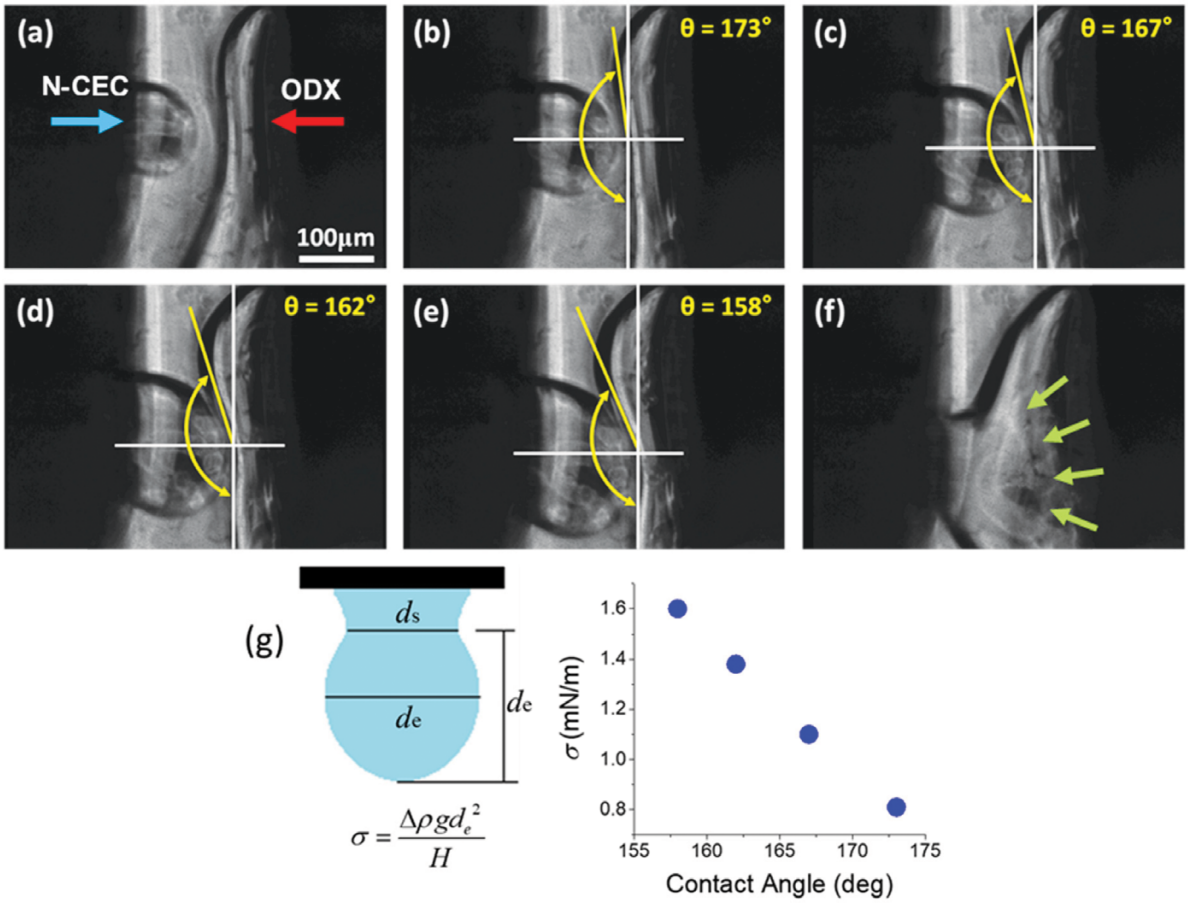

Figure 3. (a-f) The change in contact angle between the two microdroplets at the interfacial layer during the merging process. The arrows in (f) demonstrate the position of N-CEC droplet inside the merged droplet. (g) The change in surface tension (σ) of the microdroplet from (b) to (e) was calculated using the equation shown in left.

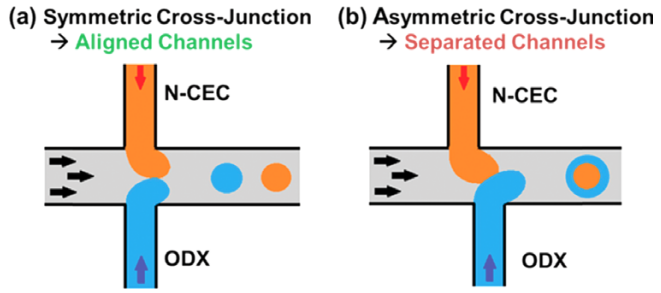

Figure 4. Mechanism of microdroplet merging at the asymmetric cross-junction. (a) In a symmetric cross-junction (channels are aligned), the emerging microdroplets directly push other, whereas (b) in a asymmetric cross-junction, one microdroplet being formed could push the other microdroplet from the side with more contact area and reduced interfacial tension for greater compression.

tion, on the other hand, one microdroplet being formed was able to push the other microdroplet from the side before spherical microdroplet was fully formed (Figure 4(b)). Therefore, the applied compression was strong enough with more contact area to overcome the reduced interfacial tension of the microdroplet, leading to the merging of the microdroplets. The difficulty of merging two droplets from a symmetric cross-junction geometry has been well documented, due to the high surface tension of droplets, thus several coalescence schemes have been introduced to actively induce merging.[33] For example, Zagnoni *et al.* applied electric field in a pulsed DC waveform to overcome the surface tension of the droplets, which led to merging of the droplets.[35] Similarly, Gu *et al.* applied magnetic field to microdroplets containing ferrofluid to induce merging.[37] However, using the asymmetric cross-junction geometry, the droplets with high and contrasting viscosities requiring the use of a high concentration of surfactant could be successfully merged without additional merging schemes.

The relative positions of the two merging channels were also optimized for proper merging of the two microdroplets. It was hypothesized that if the channels are not sufficiently separated, the two microdroplets would not be able to merge due to the insufficient level of interfacial compression unable to overcome their high surface tension. Conversely, if the channels are too far apart, then the two droplets being formed would not have enough time to contact and exert enough interfacial compression to induce merging. Therefore, the relative separation between two channels was varied up to 400 μm with 50 μm increment while keeping the flow rates constant, and the merging process was monitored. The optimal separation distance allowing the merging of the two microdroplets was determined to be 200 μm, which was used throughout this work. As expected, the separation distance below or above this value did not result in the merging.

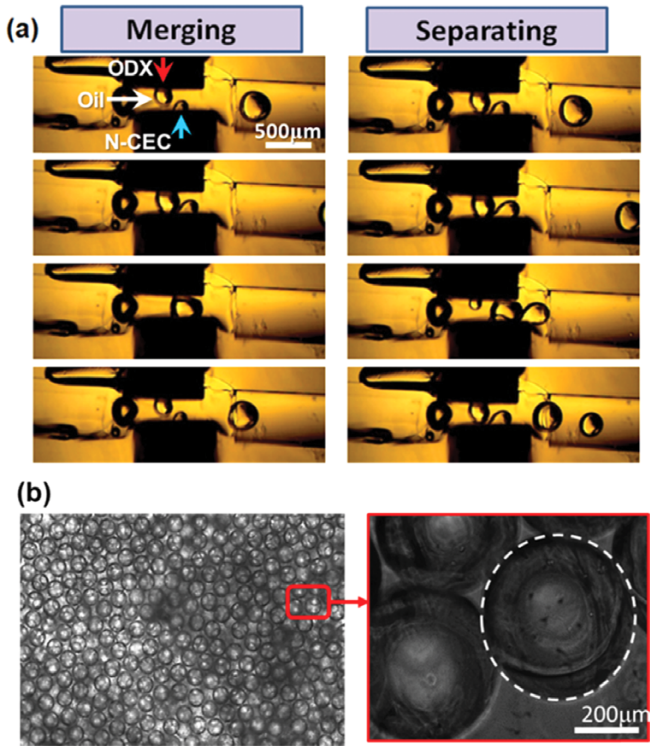

Figure 5. (a) Microscopic images of merging (left) and separation (right) of the 3% (w/v) N-CEC and 2% (w/v) ODX miscible microdroplets in an asymmetric junction; white arrow=oil in the horizontal channel; red arrow=ODX in the upper vertical channel; blue arrow=N-CEC in the lower vertical channel. (b) A microscopic image of the cell-encapsulated spherical microgels. A magnified view of a microgel is shown on the right.

Figure 5 shows the microscopic images of the merging and separation of the 3% (w/v) N-CEC and 2% (w/v) ODX microdroplets, based on different flow rates. The flow rate of the oil phase was kept at 50 μL/h, while the flow rates of ODX and N-CEC solutions were varied to find the conditions allowing the merging of two microdroplets. When the flow rates were reduced to 30 μL/h the two microdroplets stably merged to form larger microdroplets (Figure 5(a), left). On the other hand, when the flow rates were increased above 40 μL/h, the two microdroplets slipped past each other and separately passed through without merging (Figure 5(a), right)). This result demonstrated that the two forming droplets needed sufficient amount of time to break the interfacial tension between them *via* compression.

When the two miscible microdroplets were successfully merged, the N-CEC microdroplet was initially pushed into the core of the merged droplet, with the ODX microdroplet surrounding the former. As the diffusion between two layers occurred, the droplet became homogeneous, and the *in situ* gelation occurred (Figure 5(b)). It has been demonstrated that the aldehyde groups in ODX and amine groups in N-CEC undergo crosslinking reaction *via* Schiff base formation.[38,39] Under the given condition, the average diameter of the spherical microgel was determined to be 380±21 μm.

3.3. *In vitro* evaluation of biocompatibility of cell-encapsulated microgels

To investigate the biocompatibility of the *in situ* forming microgels, NIH-3T3 cells were encapsulated in the microgels prepared with 3% (w/v) N-CEC and 2% or 4% (w/v) ODX, and their viability and morphology were measured (Figure 6). In the microscopic image in Figures 6(a) and (b), the microgels crosslinked with higher ODX concentration (4% (w/v)) showed smaller diameter (433±35 μm) than those crosslinked with 2% (w/v) ODX 482±27 μm. This provided evidence of higher crosslinking density by higher concentration of ODX led to the reduced degree of swelling. The biocompatibility of the microgel was evaluated by measuring the viability of the encapsulated cells (Figure 6(c)). The cell viability in the microgels crosslinked with 2% (w/v) and 4% (w/v) ODX was determined to be 86.8 ±7.1% and 77.6±7.5% on day 0, respectively. On day 2, the viability was maintained at 81.6±5.7% and 72.2±8.6% for the 2% and 4% (w/v) ODX microgels, respectively. Although the viability was generally well maintained, there was a small decrease in viability at higher ODX concentration. This may have been due to the reduced medium perfusion into the microgel caused by the higher crosslinking density, or the increased number of aldehyde groups in ODX at higher ODX concentration causing cytotoxic effect.

4. Conclusions

In this study, a microfluidic method of merging two microdroplets with high and contrasting viscosities using an asymmetric

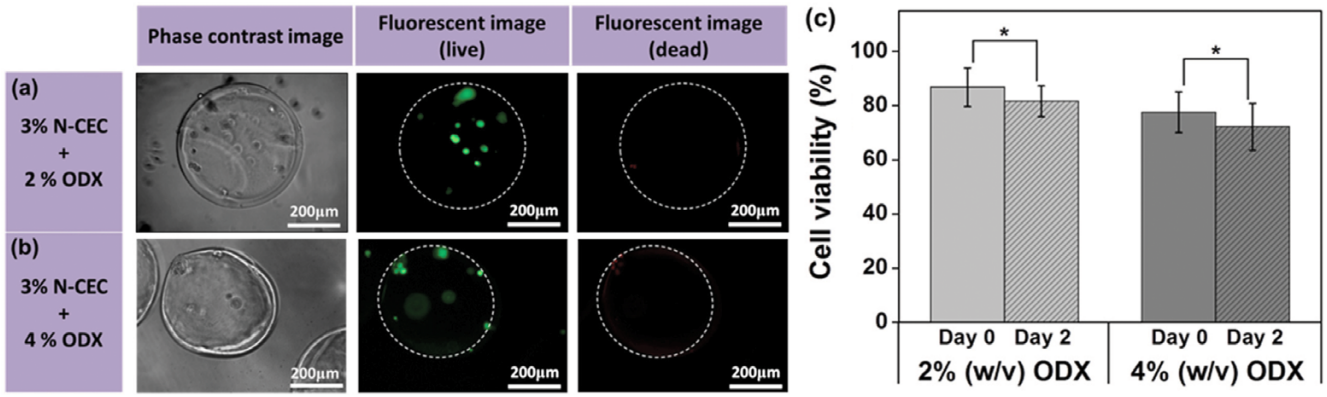

Figure 6. Phase contrast and fluorescent microscopy images of cells encapsulated in (a) 3% (w/v) N-CEC and 2% (w/v) ODX and (b) 3% (w/v) N-CEC and 4% (w/v) ODX *in situ* generated spherical microgels. (c) Cell viability measured at day 0 (right after formation) and day 2. (*P<0.01).

cross-junction geometry was introduced. The microdroplets of two viscous polymer solutions, oxidized dextran (ODX) and N-carboxyethyl chitosan (N-CEC) that can undergo crosslinking reaction to form hydrogel, was generated within the microfluidic device with the asymmetric cross-junction. In this channel geometry, the N-CEC microdroplet being formed, having higher viscosity and surface tension, exerted interfacial compressive force upon a less viscous ODX microdroplet at a position having much reduced interfacial tension. With sufficient time for the interfacial compression at reduced flow rates, the interfacial tension continued to decrease, as identified by the contact angle, until the microdroplets finally merged and became a single microdroplet. The reduced contact angle could generate sufficient shear stress to break the surfactant layer. The viscosity difference between the N-CEC and ODX monodispersed microdroplets caused the formation of core-and-shell layers at the initial stage of merging, but subsequently the two layers became fully merged *via* diffusion and microgels were formed by *in situ* crosslinking. The viability of the cells encapsulated in the microgels confirmed the biocompatibility of the microfluidic process and the resulting microgels. Overall, these results highlighted that the interfacial compression-dependent merging of the two miscible microdroplets using an asymmetric cross-junction is a promising new technology for generating in situ forming microgels from two viscous polymer solutions for various biomedical applications.

References

(1) T. Thorsen, R. W. Roberts, F. H. Arnold, and S. R. Quake, *Phys. Rev. Lett.*, **86**, 4163 (2001).
(2) C. Cramer, P. Fischer, and E. J. Windhab, *Chem. Eng. Sci.*, **59**, 3045 (2004).
(3) S. L. Anna, N. Bontoux, and H. A. Stone, *Appl. Phys. Lett.*, **82**, 364 (2003).
(4) S. A. Nabavi, G. T. Vladisavljevic, and V. Manovic, *Chem. Eng. J.*, **322**, 140 (2017).
(5) H. F. Chan, S. Ma, J. Tian, and K. W. Leong, *Nanoscale*, **9**, 3485 (2017).
(6) A. T. Tyowua, S. G. Yiase, and B. P. Binks, *J. Colloid Interface Sci.*, **488**, 127 (2017).
(7) Q. Zhang, S. Savagatrup, P. Kaplonek, P. H. Seeberger, and T. M. Swager, *ACS Cent. Sci.*, **3**, 309 (2017).
(8) S. Seiffert, M. B. Romanowsky, and D. A. Weitz, *Langmuir*, **26**, 14842 (2010).
(9) S. Y. Teh, R. Lin, L. H. Hung, and A. P. Lee, *Lab Chip*, **8**, 198 (2008).
(10) M. Sun, S. S. Bithi, and S. A. Vanapalli, *Lab Chip*, **11**, 3949 (2011).
(11) Y. C. Tan, Y. L. Ho, and A. P. Lee, *Microfluid. Nanofluid.*, **3**, 495 (2007).
(12) C. H. Yang, Y. S. Lin, K. S. Huang, Y. C. Huang, E. C. Wang, J. Y. Jhong, and C. Y. Kuo, *Lab Chip*, **9**, 145 (2009).
(13) K. Liu, H. J. Ding, Y. Chen, and X. Z. Zhao, *Microfluid. Nanofluid.*, **3**, 239 (2007).
(14) N. Bremond, A. R. Thiam, and J. Bibette, *Phys. Rev. Lett.*, **100**, 024501 (2008).
(15) B. C. Lin and Y. C. Su, *J. Micromech. Microeng.*, **18**, 115005 (2008).
(16) D. R. Link, S. L. Anna, D. A. Weitz, and H. A. Stone, *Phys. Rev. Lett.*, **92**, 054503 (2004).
(17) Y. C. Tan, J. S. Fisher, A. I. Lee, V. Cristini, and A. P. Lee, *Lab Chip*, **4**, 292 (2004).
(18) H. Sato, H. Matsumura, S. Keino, and S. Shoji, *J. Micromech. Microeng.*, **16**, 2318 (2006).
(19) B. Ziaie, A. Baldi, M. Lei, Y. Gu, and R. A. Siegel, *Adv. Drug Deliv. Rev.*, **56**, 145 (2004).
(20) S. Kim, J. Oh, and C. Cha, *Colloids Surf. B Biointerfaces*, **147**, 1 (2016).
(21) P. C. Gach, K. Iwai, P. W. Kim, N. J. Hillson, and A. K. Singh, *Lab Chip*, **17**, 3388 (2017).
(22) E. Um and J. K. Park, *Lab Chip*, **9**, 207 (2009).
(23) G. F. Christopher, J. Bergstein, N. B. End, M. Poon, C. Nguyen, and S. L. Anna, *Lab Chip*, **9**, 1102 (2009).
(24) Y. C. Tan, Y. L. Ho, and A. P. Lee, *Microfluid. Nanofluid.*, **3**, 495 (2007).
(25) S. Okushima, T. Nisisako, T. Torii, and T. Higuchi, *Langmuir*, **20**, 9905 (2004).
(26) L. Y. Chu, A. S. Utada, R. K. Shah, J. W. Kim, and D. A. Weitz, *Angew. Chem. Int. Ed.*, **46**, 8970 (2007).
(27) V. Chokkalingam, B. Weidenhof, M. Krämer, S. Herminghaus, R. Seemann, and W. F. Maier, *ChemPhysChem*, **11**, 2091 (2010).
(28) V. Chokkalingam, B. Weidenhof, M. Krämer, W. F. Maier, S. Herminghaus, and R. Seemann, *Lab Chip*, **10**, 1700 (2010).
(29) B. J. Jin, Y. W. Kim, Y. Lee, and J. Y. Yoo, *J. Micromech. Microeng.*, **20**, 035003 (2010).
(30) L. M. Fidalgo, C. Abell, and W. T. Huck, *Lab Chip*, **7**, 984 (2007).
(31) X. Niu, S. Gulati, J. B. Edel, and A. J. deMello, *Lab Chip*, **8**, 1837 (2008).
(32) J. Sivasamy, Y. C. Chim, T. N. Wong, N. T. Nguyen, and L. Yobas, *Microfluid. Nanofluid.*, **8**, 409 (2010).
(33) H. Gu, M. H. G. Duits, and F. Mugele, *Int. J. Mol. Sci.*, **12**, 2572 (2011).
(34) M. Lee, J. W. Collins, D. M. Aubrecht, R. A. Sperling, L. Solomon, J. W. Ha, G. R. Yi, D. A. Weitz, and V. N. Manoharan, *Lab Chip*, **14**, 509 (2014).
(35) M. Zagnoni and J. M. Cooper, *Lab Chip*, **9**, 2652 (2009).
(36) A. R. Guzman, H. S. Kim, P. de Figueiredo, and A. Han, *Biomed. Microdevices*, **17**, 35 (2015).
(37) V. B. Varma, A. Ray, Z. M. Wang, Z. P. Wang, and R. V. Ramanujan, *Sci. Rep.*, **6**, 37671 (2016).
(38) J. Jung, K. Kim, S. C. Choi, and J. Oh, *Biotechnol. Lett.*, **36**, 1549 (2014).
(39) L. Weng, A. Romanov, J. Rooney, and W. Chen, *Biomaterials*, **29**, 3905 (2008).
(40) J. Jung and J. Oh, *Biomicrofluidics*, **8**, 036503 (2014).
(41) J. Oh, K. Kim, S. Choi, and J. Jung, *Dig. J. Nanomater. Biostruct.*, **9**, 739 (2014).
(42) J. D. Tice, H. Song, A. D. Lyon, and R. F. Ismagilov, *Langmuir*, **19**, 9127 (2003).
(43) J. D. Berry, M. J. Neeson, R. R. Dagastine, D. Y. C. Chan, and R. F. Tabor, *J. Colloid Interface Sci.*, **454**, 226 (2015).
(44) S. Fordham, *Proc. Royal Soc. A*, **194**, 1 (1948).

